Wintertime hygroscopicity and volatility of ambient urban aerosol particles

Joonas Enroth[1], Jyri Mikkilä[1], Zoltán Németh[2], Markku Kulmala[1], and Imre Salma[2]

[1] Department of Physics, P.O. Box 64, 00014, University of Helsinki, Helsinki, Finland
5   [2] Institute of Chemistry, Eötvös University, P.O. Box 32, H–1518, Budapest, Hungary

Correspondence to: Imre Salma (salma@chem.elte.hu)

Abstract. Hygroscopic and volatile properties of atmospheric aerosol particles with dry diameters of (20), 50, 75, 110 and 145 nm were determined in situ by using a VH-TDMA system with a relative humidity of 90% and denuding temperature of 270 °C in central Budapest during two months in winter 2014–2015. The probability density function of the hygroscopic growth factor (GF) showed a distinct bimodal distribution. One of the modes was characterised by an overall mean GF of approximately 1.07 (the corresponding hygroscopicity parameter κ of 0.033) independently of the particle size, and was assigned to nearly hydrophobic (NH) particles. Its mean particle number fraction was large, and it was decreasing monotonically from 71% to 41% with particle diameter. The other mode showed a mean GF increasing slightly from 1.31 to 1.38 (κ values from 0.186 to 0.196) with particle diameter, and it was attributed to less hygroscopic (LH) particles. These hygroscopicity values are low in general. The mode with more hygroscopic particles was not identified. The probability density function of the volatility GF also exhibited a distinct bimodal distribution with an overall mean volatility GF of approximately 0.96 independently of the particle size, and with another mean GF increasing from 0.49 to 0.55 with particle diameter. The two modes were associated with less volatile (LV) and volatile (V) particles. The mean particle number fraction for the LV mode was decreasing from 34% to 21% with particle diameter. The bimodal distributions in the GF spectrum indicated that the urban atmospheric aerosol contained an external mixture of particles with a diverse chemical composition. The mean diurnal variability of the particle number fractions for the NH and LV modes, and of the volatility GF for the LV mode followed the diurnal pattern of the vehicular road traffic, while the mean diurnal variability of the hygroscopicity parameter for the NH, and of the particle number fractions for the V mode on workdays were inversely linked to the road traffic. The particles corresponding to the NH and LV modes were assigned mainly to freshly emitted combustion particles, more specifically to vehicle emissions consisting of large mass fractions of soot likely coated with or containing some water-insoluble organic compounds such as non-hygroscopic hydrocarbon-like organics. The particles related to the LH and V modes could be composed of moderately transformed aged combustion particles consisting of partly oxygenated organics, inorganic salts and soot. Both regional background sources and urban (local) emissions contribute to these particles. Dependency of the volatility GF and the volume fraction remaining after the thermal treatment on the mean hygroscopic GF suggested that the hygroscopic compounds were ordinarily volatile, and that the larger particles contained internally mixed non-volatile chemical species as refractory residuals in 20–25% of the aerosol material (by volume), which could be core-like soot or organic polymers.

1 Introduction

Aerosols influence our life and environment in multiple ways. They affect the climate system and water cycling (Boucher et al., 2013), ecosystems (Mercado et al., 2009), human health and welfare (Lelieveld et al., 2015), built environment (Brimblecombe, 2016) and visibility (Davidson et al., 2005). One of the key factors in all these processes and their consequences is the size of particles. The size distribution of atmospheric aerosol particles is primarily determined by their formation process. It can be, however, influenced further in the air by condensation or evaporation of vapours (McMurry and Stolzenburg, 1989). Water vapour is the most abundant vapour in the troposphere; it is a minor constituent of the air, while the other vapours or their precursors are present in trace concentrations. Water uptake by aerosol particles or water evaporation

from particles under subsaturated conditions (thus its hygroscopicity) are explained by Köhler theory. The interactions between water vapour and particles are affected by the size, chemical composition, surface tension and water activity of particles on one side and the meteorological conditions, specifically air temperature (T) and relative humidity (RH) on the other side. These relationships have a special climate and environmental relevance for droplet formation on cloud condensation nuclei (CCN).

5   Some particles from specific emission or formation sources contain relatively large amounts of semi-volatile chemical compounds (other than water), which can evaporate from the particles depending on ambient conditions, mainly on air T according to their partitioning between the condensed and gas phases. It is worth noting that dissolution of some atmospheric gases into droplets and their subsequent water-phase chemical reactions could also change the particle size (Meng and Seinfeld, 1994; Kerminen and Wexler, 1995). The dissolution takes place preferentially with accumulation-mode particles because of

10   the largest total surface area of this mode (and causes the splitting the accumulation mode into the condensation and droplet submodes) but the related absolute increase in the diameter is small due to the fact that the relevant gases are ordinarily present in trace concentrations, and the relative diameter increments are modest considering the diameter range of these particles. Influence of the dissolution-chemical reaction process on the particle size is smaller than that of condensation of water vapour or evaporation of semi-volatile chemical species including water, and therefore, it can be usually disregarded. The hygroscopic

15   and volatile properties have been increasingly recognised and used for global modelling purposes (McFiggans et al., 2006; Pringle et al., 2010; Rissler et al., 2010). At the same time, determination of the changes in particle size for different dry diameters under various RHs and Ts can also supply valuable indirect in situ information on the chemical composition, extent of the external or internal mixing, surface coatings and chemical reactivity of particles (Massoli et al., 2010; Wu et al., 2016). The hygroscopic properties under subsaturated conditions and volatility of ambient particles can be studied by on-line Tandem

20   Differential Mobility Analyzer (TDMA) systems, including the Volatility-Hygroscopicity TDMA (VH-TDMA). The method has particular importance since it is rather difficult to obtain direct information on the chemical composition of ambient ultrafine (UF) particles due to the small total mass represented by them, and their dynamic processes. The measurements can also be used for determining the time scales for atmospheric chemical or physicochemical transformations of freshly emitted nearly hydrophobic particles into more hygroscopic types of particles, which is a relevant issue in particular in cities. The

25   technique has been successfully applied in remote, marine, rural or semi-urban atmospheric environments worldwide, and the results and conclusions were summarised in a review paper by Swietlicki et al. (2008). Measurements on complex ambient mixtures explicitly in urban centres are more scarce (Cocker et al., 2001; Baltensperger et al., 2002; Ferron et al., 2005; Massling et al., 2005; Tiitta et al., 2010; Jurányi et al., 2013; Kamilli et al., 2014; Wu et al., 2016). In spite of the fact that the hygroscopic and volatile properties vary strongly with the location and the origin of air masses, and that urban-type air pollution

30   can strongly influence them. Moreover, multicomponent chemical mixtures of inorganic salts and organic compounds including coatings, which are typically present in ambient aerosol particles in cities, are poorly characterised and understood. The potential effects concern many people since there is a spatial coincidence between the air pollution and population density in cities.

35   As part of a long-term cooperation between the Eötvös University, Budapest and University of Helsinki in the field of atmospheric aerosol research (e.g. Salma et al., 2016b), in-situ VH-TDMA measurements were performed in central Budapest for the first time together with other supporting measurements for two months in winter. The major objectives of the present paper are to present the results on hygroscopic and volatile properties of aerosol particles with various dry diameters, to improve the geographical coverage with this type of the measurements with regard to the Carpathian Basin, to interpret the

40   two data sets jointly, to identify and discuss the mixing state and source processes of particles, and to conclude their implications on urban aerosol.

Atmospheric
Chemistry
and Physics
Discussions

2 Experimental methods

The measurements took place at the Budapest Platform for Aerosol Research and Training (BpART) research facility (Salma et al., 2016a) in Budapest from 09–12–2014 to 09–02–2015. The location represents a well-mixed, average atmospheric environment for the city centre. The sampling inlets were set up at heights between 12 and 13 m above the street level of the

5   closest road and were located in a distance of 85 m from the river Danube. Distance of Budapest to the Adriatic Sea, Baltic Sea, Black Sea and North Sea are approximately 450, 780, 830 and 1200 km, respectively. The mean and standard deviation (SD) of air T and RH inside the BpART during the measurement campaign were 20 ± 1 °C and $28\pm8\%$, respectively, and the air T stratification was avoided by extra fans located properly inside the facility. The wintertime median concentrations of elemental carbon (EC), organic carbon (OC) and particulate matter (PM) mass in the $PM_{2.5}$ size fraction were 0.97, 4.9 and 25

10     $\mu g\ m^{-3}$, respectively (Salma et al., 2017). The mean contributions of EC and organic matter (OM, with an OM/OC mass conversion factor of 1.6) to the $PM_{2.5}$ mass and SDs were $4.8\pm2.1\%$ and $37\pm10\%$, respectively, while the contribution of $(NH_4)_2SO_4$ and NH_4NO_3 derived in an earlier study in spring were 24% and 3%, respectively. The on-line instruments deployed in the present campaign were a VH-TDMA system, a differential mobility particle sizer (DMPS) system and various meteorological sensors, which were operated in parallel.

15

The key instrument related to this study was a VH-TDMA system described by Hakala et al. (2017). In short, the sample air with a flow rate of 2 L min^{-1} was dried to RH<10% using a silica-gel diffusion dried at indoor temperatures, then the equilibrium electric charge distribution of the aerosol particles was ensured by using a C-14 radioactive bipolar charger. Particles with median dry diameters of 20, 50, 75, 110 and 145 nm were preselected in a narrow quasi-monodisperse size range

20   by a 10.9-cm long Vienna-type differential mobility analyser (DMA1). The dry diameters were selected considering the shape of the particle number size distribution in Budapest to cover the Aitken and accumulation modes. The inlet air flow was then separated into two flows with equal rates, which continued to either a humidifying chamber with an enhanced RH to allow water uptake, or to a thermal denuder with a higher T to allow evaporation. The humidifier was a Gore-Tex tube with a length of 2.5 cm in a heated MilliQ water bath. The RH in the humidifier was set to 85% in the very beginning of the campaign, and

25   it was increased to 90%, which is commonly regarded as the standard humidification. The mean RH and its standard deviation (SD) were $90\pm2\%$ during the second (much longer) part of the campaign. The thermal denuder was a well-insulated cylindrical metal tube maintained at a mean temperature and SD of 270 ± 10 °C by electrical resistance wires and heat insulations. This temperature was selected by considering the thermal behaviour of relevant and abundant inorganic salts, several types of organic compounds and soot (Park et al., 2009; Hakala et al., 2017) and previous experience with ambient aerosol particles

30   (Tritscher et al., 2011; Hong et al., 2014). Atmospheric sulphates, nitrates and most organics are usually volatile at this temperature, while soot (and some organic polymers) remain refractory. The two main classes can be advantageously combined with the hygroscopicity measurements. The centreline residence times of particles in the humidifying section and thermal denuder were 0.6 and 0.5 s, respectively, which is adequate for equilibrium particle growth/evaporation of typical inorganic salts (Chan and Chan, 2005). The humidifier and denuder were operated in parallel, giving simultaneous data on hygroscopic

35   and volatile properties of particles. The advantage of this combination is a better time resolution, which is an important factor for relatively rapidly varying urban atmospheric environments. The changes in particle diameter after the humidifier were determined by a Vienna-type DMA (DMA2a) with a length of 28 cm and a condensation particle counter (CPC, TSI, model 3772, operated with an option of water removal on). The sheath air flow of the DMA2a was also humidified to the selected RH. The changes in particle diameter after the thermal denuder were measured by a Vienna-type DMA (DMA2b) with a length

40   of 10.9 cm and a CPC (TSI, model 3010). The concentration of the size-selected particles in the denuded air flow was low enough to prevent recondensation after the denuder (Park et al., 2009). The T and RH of the air flows were monitored just at the entrance to the second set of DMAs. The RH was measured by using a chilled-mirror dew point hygrometer located in the excess air flow of the DMA2a. The DMA1, DMA2a and DMA2b were all operated with a closed loop sheath air flow system

with flow rates of 20, 10 and 9 L min^{-1}, respectively. The time resolution of the VH-TDMA system was 18 min. Calibration, quality check of the hygroscopic GF and operation check of the volatility GF for all selected diameters was performed by nebulising dilute solution of analytical grade $(NH_4)_2SO_4$ into the filtered inlet air flow of the VH-TDMA system. The system was operated according to international recommendations (Massling et al., 2011).

5

The DMPS used was a flow-switching type system (Salma et al., 2011b; Salma et al., 2016a). Its main components are a radioactive (Ni-60) bipolar charger, a Nafion semi-permeable membrane dryer, a 28-cm long Vienna-type DMA and a butanol-based CPC (TSI, model 3775). It measures particle number size distributions in an electrical mobility diameter range from 6 to 1000 nm in the dry state of particles (with a RH<30%) in 30 channels with a time resolution of approximately 8 min. The

10 sample flow rate is 2.0 L min^{-1} in high-flow mode, and 0.30 L min^{-1} in low-flow mode with sheath air flow rates 10 times larger than for the sample flows. The DMPS measurements were performed according to the recommendations of the international technical standard (Wiedensohler et al., 2012). Weather shield and insect net were adopted to both aerosol inlets. The meteorological data were available from Urban Climatological Station of the Hungarian Meteorological Service operated at a height of 10 m above the roof level of the building (at a height of 39 m above the ground) in a distance of about 40 m from

15 the BpART facility, and from a simpler on-site meteorological station. Standardised meteorological measurements of T, RH, wind speed (WS) and wind direction (WD) were recorded with a time resolution of 10 min.

3 Data evaluation

The ratio of the particle diameter after the treatment in the humidifier or thermal denuder to the initially selected diameter is the diameter growth factor (GF). It expresses both possible growth and shrinkage of particles. For ambient particles, the GFs are

20 spread in a distribution, which was measured by holding the particle size selected by the DMA1 constant, and scanning by the second set of DMAs (DMA2a and 2b) through possible diameter ranges that correspond to humidity GFs from 0.9 to 2.0, and to volatility GFs from 1.3 to 0.3. This resulted in a distribution of the GF, which is referred as GF probability density function (GF-PDF). It is, however, a smoothed and skewed form, which needs to be mathematically inverted to derive the distribution accurately since the transfer function of the second set of DMAs has a finite width, and since their total transfer

25 probabilities depend on the classifying voltage and operational parameters of the DMA (Swietlicki et al., 2008; Gysel et al., 2009). The inversion process yields the true GF-PDF for each scan, and it is also normalised to unity. The inversion was accomplished by applying the program package TDMAinv (Gysel et al., 2009) in IGOR Pro software. The program package was shown to be robust, appropriate and adequate in several previous studies (e.g. Liu et al., 2011; Hong et al., 2014). The hygroscopic property was also expressed by hygroscopicity parameter (κ value, Petters and Kreidenweis, 2007). The κ value

30 is a compound parameter with more sophisticated interpretation than the hygroscopic GF, but it can be used in the Köhler model as proxy for the chemical composition without explicitly knowing the density, molecular mass, van't Hoff factor and osmotic coefficient or dissociation number of each chemical component. It was calculated for each GF as:

$$\kappa = (GF^3 - 1)\left[\frac{1}{S}\exp\left(\frac{4\sigma M_w}{RT\rho_w D_d GF}\right) - 1\right], \tag{1}$$

where S is the saturation ratio of water (S=RH, when RH is expressed as a fraction), σ is the surface tension of the droplet-air

35 interface at the composition of the droplet, M_w is the molecular mass of water, R is the universal gas constant, T is the droplet temperature, ρ_w is the density of water in the droplet, and D_d is the dry diameter of the particle. The σ was assumed to be that of pure water (σ=72 mN m^{-1} at 20 °C). It was shown that some organic chemical species in atmospheric aerosol particles such as humic-like substances (HULIS) are surface active and can lower the surface tension of the water droplet (Facchini et al., 1999; Salma et al., 2006). The use of a smaller σ than for pure water yields smaller κ values. The depression of σ in time is

Atmospheric
Chemistry
and Physics
Discussions

controlled by diffusion of HULIS from the bulk of the droplet to its surface, and it takes several hours to reach the thermodynamic equilibrium at medium concentrations (Salma et al., 2006). This also means that the extent of the actual decrease is kinetically limited to larger than equilibrium values, and therefore, the utilisation of $\sigma=60$ mN m^{-1} is expected to represent a lower estimate. The κ values obtained by this surface tension changed by a mean factor of 0.97–0.98 for particles

5   with a diameter of 70, 110 and 145 nm, while the mean factor for particles with a diameter of 50 nm became 0.95. This all implies that the alterations related to the lower surface tension than that of water are small with respect to experimental uncertainties, and that the calculations with σ for water seem to be a sensible approach to reality. This is also confirmed in an earlier study, according to which the influence of σ seems small under subsaturated conditions (Swietlicki et al., 2008). The soluble particle volume fraction is used conventionally to classify different groups of hygroscopic growth in order to facilitate

10   data comparability. Here, we utilised different κ values and GFs to define commonly observed hygroscopic groups (Liu et al., 2011). The limits of the groups are, however, not exactly determined, and are often set as 1) $\kappa \leq 0.10$ (GF$\leq$1.21): nearly hydrophobic (NH) particles; 2) $\kappa \approx 0.10$–0.20 (GF=1.21–1.37): less hygroscopic (LH) particles, and 3) $\kappa > 0.20$ (GF$>$1.37): more hygroscopic (MH) particles. The GFs above refer to particles with a diameter of 100 nm and RH=90%, and they vary with D_d and RH. On one side, small values of κ indicate low CCN-active behaviour. As κ approaches 0, the particle resemble an

15   insoluble but wettable particle. On the other side, the upper limit for the most hygroscopic species typically found in the marine atmospheric aerosol particles (e.g. NaCl) is $\kappa \approx 1.4$ (GF$>$1.85; Petters and Kreidenweis, 2007).

The volume fraction remaining (VFR) after the thermal treatment was calculated from the volatility GF assuming spherical shape of particles both before and after the treatment (Häkkinen et al., 2012). Diurnal variability for a selected variable was

20   derived by averaging the measured data for the corresponding hour and then by averaging the hourly means for the whole time interval. Evaluation of the measured DMPS data was performed according to the procedure protocol recommended by Kulmala et al. (2012). Mathematically inverted DMPS data were utilised for calculating particle number concentrations in the particle diameter ranges from 6 to 100 nm ($N_{<100}$), from 100 to 1000 nm ($N_{>100}$) and from 6 to 1000 nm (N). Median particle number size distribution was derived from the individual concentration data.

25   **4 Results and discussion**

Most of the measurement period consisted of mild and moist winter weather. The air T and RH ranged from −9 to 17 °C, and from 40 to 99%, respectively with means and SDs of 3.0±4.2 °C and 84±13%, respectively. No extreme wind conditions were encounter; the mean WS and its SD were 1.9±1.7 m s^{-1}. The median N and UF particle number concentration were 5.0×10^3 cm^{-1} and 4.1×10^3 cm^{-1}, respectively, and the mean UF/N concentration ratio and its SD were 82±9%. These median

30   concentrations are below the annual medians (Salma et al., 2016b). There were four quantifiable new aerosol particle formation (NPF) and growth events identified in the DMPS data set during the VH-TDMA measurement campaign in winter. Unfortunately, only one of them was fully covered by the VH-TDMA system, and therefore, no representative conclusion can be drawn for them (cf. Kerminen et al., 2012; Wu et al., 2016).

4.1 Growth factor spectra and their temporal variability

35   Time series of the hygroscopic GF-PDF for particles with a dry diameter of 145 nm and particle number concentrations in various size fractions for approximately 1 week are shown in Fig. 1 as example. The white bands indicate missing data which were caused by problems in data recording of the VH-TDMA system. The GF-PDF exhibited persistently existing bimodal distribution. The mode with the smaller GF values represents nearly hydrophobic (NH) particles, while the other mode with the larger GFs is related to less hygroscopic (LH) particles. The two modes were constantly present and were well separated

40   during the whole campaign despite the large variations in N and $N_{>100}$ concentrations. Fig. 1 also confirms that the classification

of the NH and LH hygroscopic groups (see Sect. 3) was appropriate. The contribution of the two modes was size dependent. The NH mode decrease with particle size. The smallest, 20-nm particles already resembled unimodal NH distribution for most of the time. Two distinct modes showed up in the volatility GF-PDF spectrum as well, and they were also constantly present during the whole campaign. The mode with the volatility GF>0.8 was assigned to less volatile (LV) particles, while the mode

5   exhibiting GF≤0.8 was associated with volatile (V) particles. The bimodal distributions indicated that the particles had separate chemical composition, thus they were present in external mixture, except for 20-nm particles, which basically showed internal mixture of constituents. The relative contribution of the modes were highly variable, which can be explained by the temporal variability in the intensity of the major emission and formation sources of the corresponding particles, in their atmospheric transformation processes, and by the influence of different air masses.
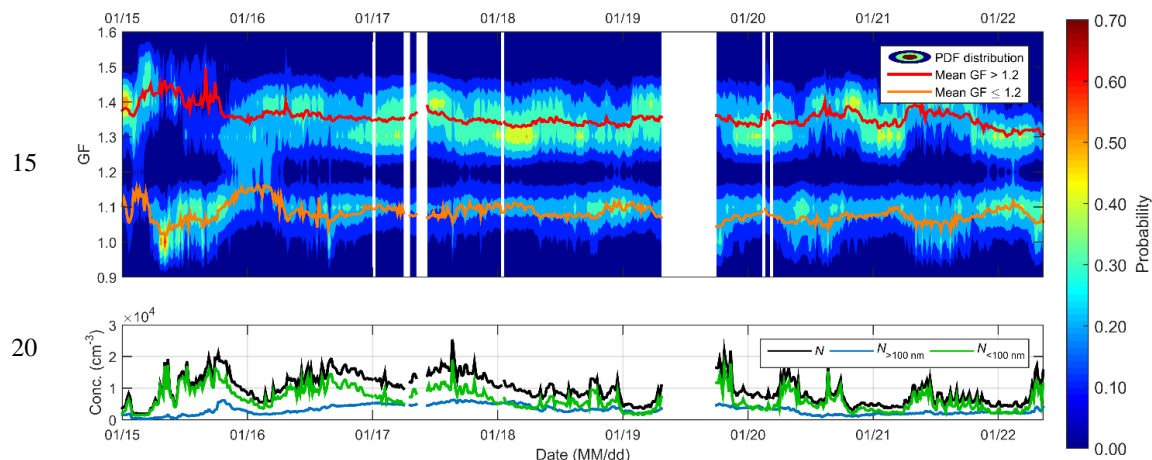
10

Figure 1. Temporal variability of the hygroscopic diameter growth factor probability density function (GF-PDF) (upper panel) at RH=90%
25   for particles with a dry diameter of 145 nm from 15 to 22 January 2015. The orange line represents the mean GF of the nearly hydrophobic mode, while the red line shows the mean GF of the less hygroscopic mode. The total particle number concentration (N, black line), and concentrations of $N_{<100}$ (green line) and $N_{>100}$ (blue line) are also shown on the lower panel.

4.2 Averages of hygroscopic and volatile properties

30   Median particle number size distribution together with the mean hygroscopic GF-PDF and the mean volatility GF-PDF for the selected particle diameters are shown in Fig. 2. The broadening of the size distribution (Fig. 2a) was caused by the averaging the individual data. Fig. 2a shows that the selected diameters of 20, 50, 75, 110 and 145 nm represent the plateau of the size distribution, and that the median ambient concentrations of these particles were very similar to each other. The particles with a diameter of 20 nm were omitted from the volatility evaluation and Fig. 2c because they appeared at the lower end of the GF

35   range after the shrinkage, thus their diameters were close to the detection limit of the CPC (TSI model 3010) used as the detector, and they were also subjected to enhanced diffusional losses. The mean GF distributions for humidity and volatility clearly exhibited bimodal character. The relative contribution of NH mode in the hygroscopic GF-PDF (Fig. 2b) was decreasing with particle diameter, while there was no similar obvious tendency for the volatility GF-PDF (Fig. 2c).
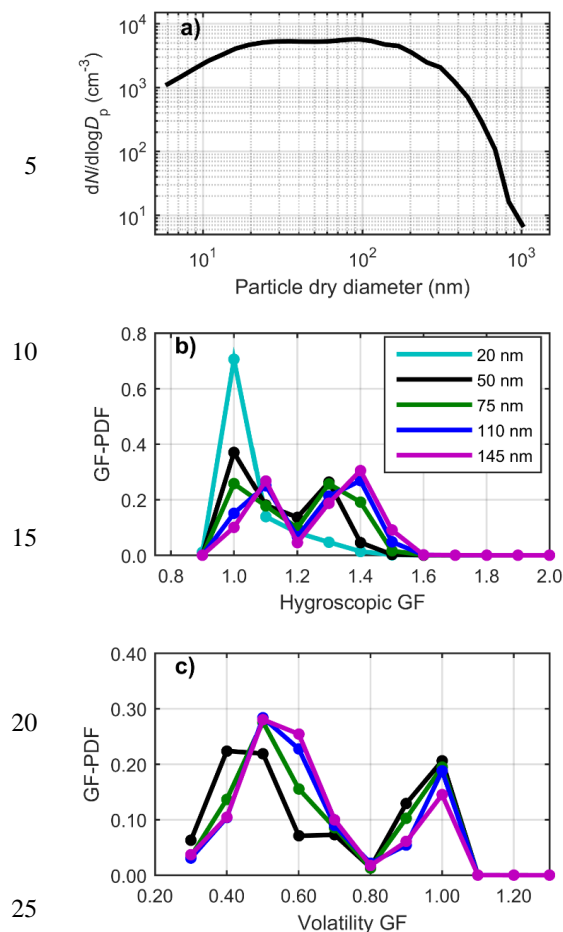
Figure 2. Median particle number size distribution for the whole campaign (a) together with the mean hygroscopic diameter growth factor probability density function (GF-PDF, b) and volatility diameter GF-PDF (c) for different dry particle diameters. The panels b and c have shared legends.

The mean hygroscopic GFs and κ values separately for the NH and LH modes, and the mean volatility GFs separately for the LV and V modes together with the relative concentrations of particles in each mode for the selected dry diameters are summarised in Table 1. Relatively small size dependency was observed for the growth of the NH and LH modes as well as for the shrinkage of the LV and V modes, while the relative particle number concentration of the modes varied substantially. Specifically, the mean GF for the NH mode of approximately 1.07 did not seem to depend on particle size, while the mean particle number fraction for the NH mode decreased monotonically and substantially, from 71% to 41% with particle diameter. It is mentioned that more than 85% of particles with a diameter of 20 nm were associated with the NH mode, and they showed the largest time variation. The slight change in the hygroscopic growth behaviour cannot be reliably interpreted without measurements at high (>95%) RHs. The situation was similar for the LV mode, thus the mean GF stayed constant at approximately 0.96 independently of the particle size, while the particle number fraction in the mode was decreasing, although its extent was less pronounced, from 34% to 21%. The NH mode and the LV mode were related to freshly emitted combustion particles consisting of large mass fractions of soot and some water-insoluble organic compounds (Liu et al., 2013). The latter species can be a mixture of non-hygroscopic Hydrocarbon-like Organic Aerosol (HOA) in the condensed phase and adsorbed Volatile Organic Compounds (VOCs) in a huge number from the gas phase. The tendencies in the hygroscopic and volatile properties, and in the particle number fraction of modes mentioned above are ordinarily observed in urban VH-TDMA studies

Atmospheric
Chemistry
and Physics
Discussions

(e.g., Ferron et al., 2005) since the particle number size distribution of soot from traffic emissions peaks between 50 and 100 nm (Weingartner et al., 1997). It was previously concluded that uncoated fresh soot particles (although of somewhat larger diameters than 145 nm) showed neither hygroscopic growth nor water activation, while their coating with succinic acid, sulphuric acid or polyaromatic hydrocarbons (PAHs) influenced the hygroscopic growth in a complex way (Henning et al.,

5   2012). The diameter change depended on the amount and type of the coatings, on the "humidity history" of particles (coating by solution layer or solid film) and on the carrier gas used in the experiments. The interaction also included hygroscopic shrinkage. Hygroscopic GFs up to 1.11 were obtained with succinic acid at 98% RH for particles with 375 and 500 nm dry diameter (Henning et al., 2012). It has to be noted that succinic acid coating on soot particles appears to be a good example for oxygenated organic substances in atmospheric environments strongly influenced by biogenic activities, while the situation

10   with the coatings in urban environments can be different. Atmospheric fresh soot agglomerates have fractal structure, which can be reconstructed when exposed to high RH due to capillary condensation or to filling of cavities leading to compaction (Weingartner et al., 1995). The particles after the structural change (collapse) become less fractal or more compact, which results in decreased electrical mobility diameter, and thus leads to shrinkage (hygroscopic GF<1) or underestimated hygroscopicity obtained by diameter-based methods. The restructuring has been observed for different soot types (Weingartner

15   et al., 1995; Tritscher et al., 2011) and for particles with a D_d >100 nm (Martin et al., 2012). The hygroscopic GF for the LH mode increased monotonically and in a modest way (from 1.31 to 1.38) with particle size, while the fraction of particles in the LH mode increased with diameter from 29% to 59%. It is worth realising that the GFs for pure $(NH_4)_2SO_4$ and NH_4NO_3 (Park et al., 2009) are substantially larger than the measured values, which indicate considerable abundance of less hygroscopic species that are internally mixed with the inorganic salts. These particles can be composed of moderately transformed aged

20   soot-containing combustion particles comprising also partly oxygenated organics and inorganic salts (Duplissy et al., 2011; Liu et al., 2013). This view is further confirmed by a high-resolution TEM/EDS study of individual particles at the BpART facility (Németh et al., 2015). Both regional background sources and urban (local) emissions contribute to these particles (Swietlicki et al., 2008), which can result in more complex situations. The whole explanation is also consistent with the fact that the mixing state of soot particles is largely determined at their sources (Liu et al., 2013). The relative concentration of V-

25   mode particles was increased from 66% to 79% with diameter, and this was accompanied by a modest decrease in volatility.

Table 1. Mean hygroscopic growth factor (GF) and mean hygroscopicity parameter (κ) separately for nearly hydrophobic (NH) mode (GF<1.2) and less-hygroscopic (LH) mode (1.45>GF≥1.2) obtained for different particle diameters (D_d) at the mean RH and SD of 90±2%, and mean volatility GFs separately for less volatile (LV) mode and for volatile (V) mode observed at the mean temperature and SD of 270±10 °C. Mean relative contribution of particles to the total particle number concentration (nf., number fraction in %) and SD for each

30   mode are also given.

| D_d | 50 nm | | 75 nm | | 110 nm | | 145 nm | |
Mode	Mean	SD	Mean	SD	Mean	SD	Mean	SD
NH GF	1.07	0.04	1.07	0.04	1.09	0.03	1.09	0.03
NH nf.	69	17	53	16	47	13	41	11
NH κ	0.034	0.020	0.033	0.018	0.037	0.015	0.037	0.012
LH GF	1.31	0.02	1.35	0.03	1.37	0.03	1.38	0.04
LH nf.	31	17	47	16	53	13	59	11
LH κ	0.190	0.015	0.197	0.019	0.20	0.02	0.20	0.03
LV GF	0.96	0.02	0.96	0.02	0.97	0.02	0.96	0.02
LV nf.	34	17	30	16	24	14	21	12
V GF	0.49	0.05	0.52	0.04	0.54	0.04	0.54	0.04
V nf.	66	17	70	16	76	14	79	12

The hygroscopic GFs observed in Budapest correspond to the results reported for other urban areas (Cocker et al., 2001; Baltensperger et al., 2002; Ferron et al., 2005; Massling et al., 2005; Swietlicki et al., 2008 and references therein; Laborde et al., 2013; Lance et al., 2013; Ye et al., 2013); our data are slightly below the average GFs. Laborde et al. (2013) further

Atmospheric
Chemistry
and Physics
Discussions

observed that the fresh traffic emissions have virtually hydrophobic behaviour, which is also close to our conclusion on the NH mode. The studies also reported the presence of a MH mode, which was not present in our data set. This mode is attributed in most cases either to the aged continental mostly soot-free background aerosol particles (Liu et al., 2013) entering the urban air or to particles from efficient biomass burning (BB; Swietlicki et al., 2008). The missing MH mode in the Budapest data

5   suggests that the particles from local urban and rural regional sources seem more important inside the city than that from continental background sources, and the distance from the sea can possibly play a role as well. This is in line with the decreasing tendency in the annual mean UF particle number concentration and SD from the city centre ($8.4 \pm 5.3 \times 10^3$ cm^{-3}) through the near-city background ($3.1 \pm 2.8 \times 10^3$ cm^{-3}) to the rural background ($3.8 \pm 3.6 \times 10^3$ cm^{-3}; Salma et al., 2014, 2016b), and with the estimated total concentrations for the continental background up to 500–800 cm^{-3} (Raes et al., 2000). As far as the BB is

10   concerned, it was recently estimated that the mean contribution and SD of OC from BB to the total carbon in central Budapest in winter was the largest single value of $34 \pm 8\%$, with contributions from fossil fuel combustion and biogenic emissions of $25 \pm 6\%$ and $24 \pm 9\%$, respectively (Salma et al., 2017). The particles emitted from high-temperature efficient BB are rich in alkali salts and contain depleted amounts of organic compounds, thus they are expected to be very hygroscopic (Mircea et al., 2005; Rissler et al., 2005). The absence of the MH mode in Budapest could indirectly imply that the BB in the area likely took

15   place as low-temperature incomplete combustion of biofuels, which produces organic aerosol constituents with limited water uptake. This hypothesis, however, needs to be further studied.

4.3 Diurnal variability

Mean diurnal variability of the particle contributions to the NH and LV modes (Fig. 3) showed relatively large change during the day, and displayed a shape which corresponds to the typical daily-activity time pattern of inhabitants in cities, including

20   particularly the road traffic in Budapest (Salma et al., 2011a). It consists of two peaks at approximately 8:00 and 18:00, which coincide with the most intensive vehicle traffic (morning and afternoon rush hours). This diurnal pattern of the modes was also strongly correlated with the total particle number concentration (with correlation coefficients of $R= -0.907$ and -0.882 for the NH and LV modes, respectively), which is influenced by the traffic emissions (Salma et al., 2014). Since the rush hours also coincided with the sunrise and sunset in winter, the sun elevation angle was calculated, and it was compared to the diurnal

25   pattern of the LV mode. It was found that the fraction of the LV mode began to elevate before the sunrise, and hence, before boundary layer mixing or photochemistry could take place. This all suggests that the NH and LV modes are related to the direct emissions from road vehicles.

The diurnal variability in the hygroscopicity was more complex. The mean diurnal dependency of the κ value for all data, and

30   separately for the NH mode and LH mode are shown in Fig. 4. The diurnal pattern of the κ value for all data (Fig. 4a) showed the largest values during the early morning hours. This is different from those found in other studies in urban air. Lance et al. (2013) and Bialek et al. (2014) observed larger mean κ value than in the present work, and its diurnal variability was different. The lowest hygroscopicity occurred in the early morning hours (around 5:00), followed by a steady increase until the early afternoon, when it started to decrease towards the early morning minimum. These differences can be likely explained by the

35   fact that the locations of the previous studies cannot be regarded strictly as city centre, and a strong natural aerosol component could be present. This further is supported by the fact that the diurnal cycles they found are similar to those obtained for a remote site at Hyytiälä, Finland (Ehn et al., 2007). The diurnal hygroscopicity curves for the NH mode (Fig. 4b) were anti-correlated with the diurnal variation of the traffic intensity (and with the fraction of particles in the NH mode, cf. Fig. 3a). This imply that the variation of hygroscopicity of the NH mode was largely due to the diurnal variation of the number fraction of

40   NH particles, thus the change was dominated by the emission sources. Our κ values also agree well with the findings for fresh and aged particles emitted from a diesel engine (Tritscher et al., 2011). Hygroscopicity parameters for the LH mode were larger during the daylight time period than for the night. Its diurnal variation resembles the shape found in other urban studies

Atmospheric
Chemistry
and Physics
Discussions

(Kitamori et al., 2009; Massling et al., 2005). For 50-nm particles, the LH mode displayed somewhat different shape, which indicates that these particles could have different composition from the other particles. It is also seen that the overall hygroscopicity (Fig. 4a) shows more sensitive size dependency than the diurnal patterns for the NH mode (Fig. 4b) and LH mode (Fig. 4c). This means that the mean κ values were more influenced by the fraction of particles in each mode than by the size-dependent changes in the chemical composition.

Figure 3. Mean diurnal variability of the relative concentration of particles in the nearly hydrophobic (N_{NH}/N) mode (a) and less volatile (N_{LV}/N) mode (b) for different particle diameters. The panels have shared legends.
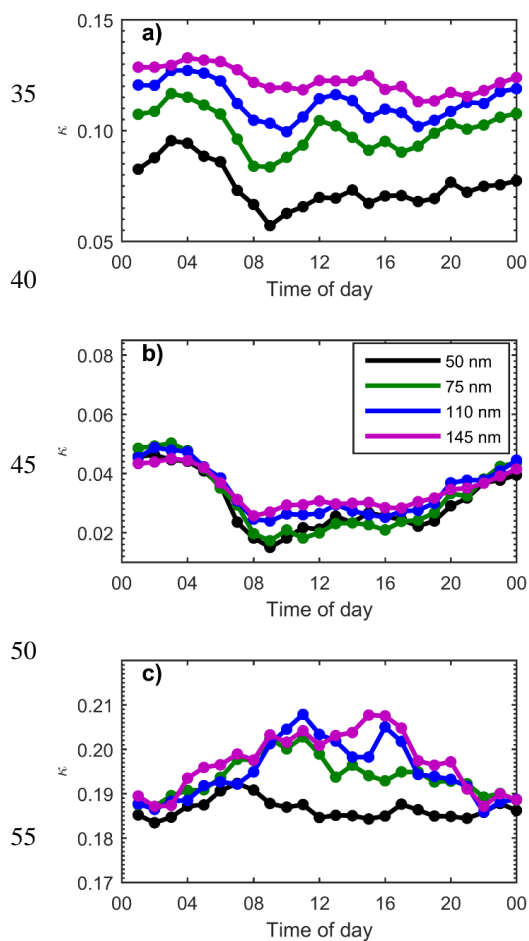

Figure 4. Mean diurnal variability of the hygroscopicity parameter κ for all data (a), separately for the nearly hydrophobic mode (b) and less hygroscopic mode (c) for different particle diameters. The panels have shared legends.

The volatility GF for the LV mode showed a clear daily-activity time pattern (Fig. 5a). This implies that the LV mode was also influenced by the vehicle road traffic. Particles with diameters of 50 and 70 nm seemed more volatile during the daylight time period than the 110- and 145-nm particles. The latter two sizes are in the typical size range of fresh diesel emissions (Charron and Harrison, 2003), and this can explain their lower volatility. These particles also had a larger magnitude in the GF daily variability than the smaller particles. This indicates that the larger particles in the LV mode had more variation in their composition, and could consist of fresh non-volatile traffic emissions which collected or adsorbed condensing organics on their surface. For the volatile mode (Fig. 5b), no obvious diurnal pattern was observed for any particle diameter. The associated particles showed more or less constant GFs during the day. Particles with a diameter of 50 nm exhibited larger volatility (GF<0.5) than for the other diameters, while particles with diameters of 110 and 145 nm showed almost identical volatile properties.
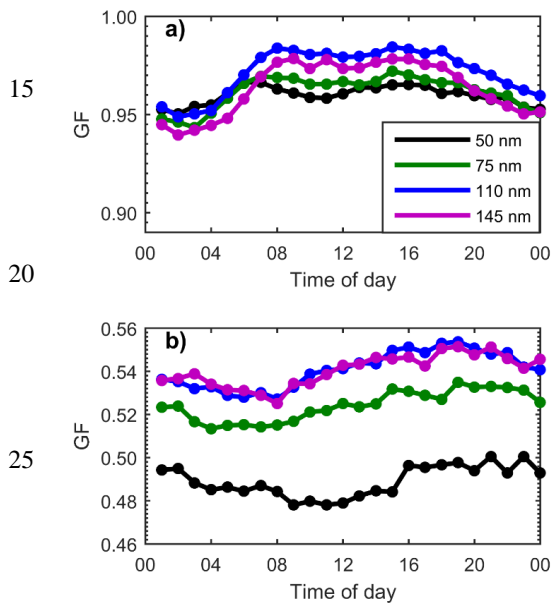

Figure 5. Mean diurnal variation of the volatility diameter growth factors for the less volatile mode (a) and volatile mode (b) for different particle diameters. The panels have shared legends.

4.4 Relationships between workdays and weekends

The overall influence of vehicle emissions on the hygroscopicity and volatility of particles were studied by evaluating the data set separately for workdays and weekends since there is less vehicular road traffic during the weekends than on workdays (Salma et al., 2011a), and since the atmospheric residence time of the particles with the selected diameters is estimated to be several hours. Diurnal variability of the total particle number concentration, fraction of particles in the volatile mode, and of the hygroscopicity parameter of the NH and LH modes for workdays and weekends are shown in Fig. 6. It is seen in Fig. 6a that the N increased monotonically and rapidly from 5:30 to 7:00 on workdays, and reached its first maximum between 7:00 and 8:00. The concentration remained at elevated level over the whole daytime period. A second broader maximum appeared at around 18:00, and the N decreased monotonically after this peak till about 4:00 next morning. On weekends, the morning growth was slower, and the first maximum was shifted to approximately 11:00, and its amplitude was much smaller. The remaining part of the curve was similar in shape to that for workdays but reached considerably smaller levels than on workdays.

These are in good agreement with ordinary vehicular traffic flow in central Budapest (Salma et al., 2011a) except for the fact that the mean traffic flow from 0:00 to 5:00 is usually larger on weekends than on workdays. This latter difference can be likely explained by the changes in the composition of the vehicle fleet on workdays and weekends (less buses and heavy-duty vehicles on weekends and particularly overnights). Influence of the road traffic was clearly manifested in the diurnal variation

5 of the number fraction of particles in the volatile mode (Fig. 6b), which essentially varied inversely with N and traffic intensity. This probably indicated less variability in or constant shape of the N_V concentration during the day. The extent of the decrease for the morning and evening rush hours decreased monotonically with the particle diameter. The hygroscopicity parameters for the LH mode on workdays or on weekends (Fig. 6c) were similar to each other. Except for the particles with a diameter of 50 nm, for which the κ value was small, comparable to each other in their extent, and without evident diurnal variability for

10 both workdays and weekends. For the other diameters, the κ values on workdays were somewhat larger, but without substantial variation during the daylight period. For weekends, the hygroscopicity parameters reached their largest value in the early morning hours, and seemed to be somewhat larger than for the workdays. The diurnal variability curves for the hygroscopicity of the LH mode were similar to each other separately for workdays and for weekends (Fig. 6d). The curves showed an inverse shape with N and traffic intensity (cf. Fig. 6a). There was a larger decrease in the hygroscopicity parameter in the morning

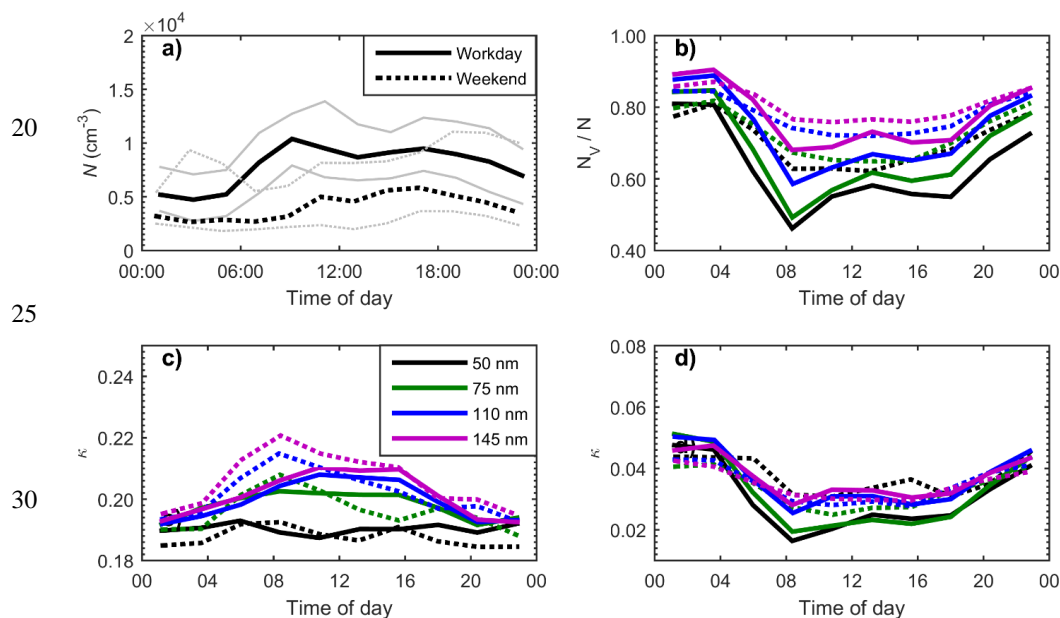15 rush hours for workdays than for weekends, in particular for particles with diameters of 50 and 75 nm.

Figure 6. Diurnal variability of the median total particle number concentration (N, panel a), mean number fraction of particles in the volatile

35 (N_V/N) mode (b), and the mean hygroscopicity parameter of the less hygroscopic mode (c) and nearly hydrophobic mode (d) separately for workdays (solid lines) and weekends (dotted lines). The thin lines in grey on panel a represent the lower and upper quartiles of the corresponding concentration data. The panels b, c and d have shared legends.

4.5 Conjugate hygroscopic and volatile properties

40 Relationships between hygroscopic and volatile properties were studied by relating their mean values to each other directly (Fig. 7 upper panel) and by deriving the mean volume fraction remaining (VFR) from the particles after the thermal treatment as function of the mean hygroscopic GF (Fig. 7 lower panel). Both the volatility GF and VFR decreased monotonically with the hygroscopicity of particles. The relationships were size dependent, which may indicate that there were different abundances

Atmospheric
Chemistry
and Physics
Discussions

and/or different chemical species of organic compounds in the particles of different dry diameters. A levelling off tendency was observed for particles with diameters of 110 and 145 nm at larger hygroscopic GF values, and they also started behaving similarly to each other. The VFR dependency for these two particle diameters seemed to be also limited from the bottom at approximately 25%. This all suggests that the volatile and hygroscopic properties varied in a coherent manner, that the

5   hygroscopic compounds were volatile, and that the larger particles contained internally mixed non-volatile chemical species in a considerable volumetric ratio as refractory residual, which could be core-like soot or organic polymers.
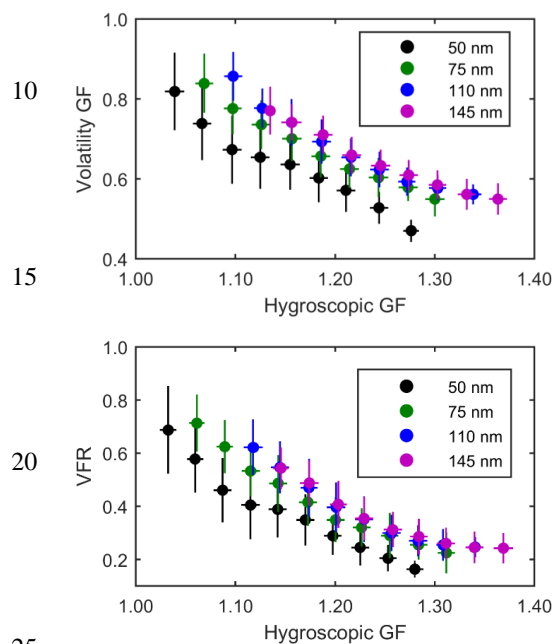

Figure 7. Relationship between the mean hygroscopic growth factors (GFs) and the conjugate volatility GFs (upper panel), and between the hygroscopic GFs and the conjugate volume fraction remaining (VFR) after the thermal treatment (lower panel) obtained at a mean relative humidity and at a mean temperature of 90% and 270 °C, respectively. The error bars indicate ±one standard deviation.

30   There were further important links between the modes of the hygroscopicity and volatility PDFs. Figure 8 shows the mean diurnal variability of κ-PDF and volatility GF-PDF for various dry diameters. It is worth mentioning that the colour coding depicts the normalized concentration fractions, and not the absolute concentrations. For instance, the decrease in the volatile mode during the daytime was caused by the appearance of larger number of less volatile particles. The NH mode consisted of a mixture of particles with a $\kappa<0.05$ and a $\kappa\approx0.05$. The smallest particles (with dry diameters of 50 and 75 m) appeared to be

35   dominated by vehicle emissions since their size range, diurnal variability and timing matched the traffic intensity and emissions. Furthermore, the corresponding occurrence of the LV mode (Fig. 8 lower panels) supports the conclusion that road traffic was a major source of these particles. The NH mode for the larger particles was likely associated with a mixture of aged particles from traffic sources and biomass burning emissions as they are present during the day (Salma et al., 2017), and still show considerably low hygroscopicity. For the LH mode, the intermodal variation was less apparent. This mode showed a

40   diurnal variation with a daytime maximum, which is similar to that observed for the overall hygroscopicity at rural sites (Ehn et al., 2007). The intermodal variability for volatility GFs can be explained by a constant background of volatile particles and by a varying contribution from less volatile particles from traffic emission. The midday decrease in the probability density function in the volatile mode was again due to the appearance of less volatile particles (the concentration of the volatile particle background did not change substantially) likely originating from traffic.
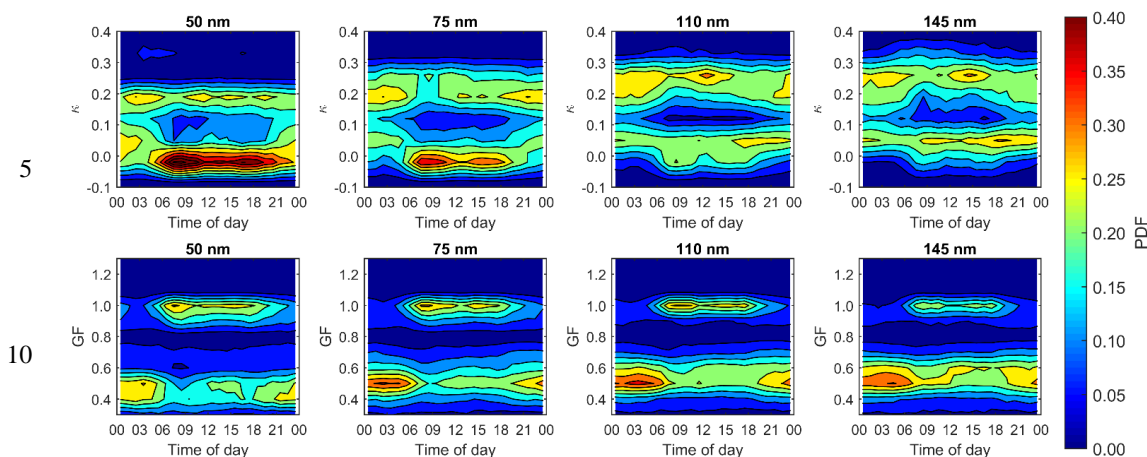
Figure 8. Mean diurnal variability of hygroscopicity parameter κ and volatility growth factor (GF) probability distribution functions (PDFs) for particles with dry diameters of 50, 75, 110 and 145 nm. The negative κ values are an artefact of plotting the data.

5 Conclusions

Hygroscopic GFs, volatility GFs and hygroscopicity parameters were quantified for ambient aerosol particles with dry diameters of (20), 50, 75, 110 and 145 nm in situ by using a VH-TDMA system in central Budapest during two months in winter. The measurements were supported by a DMPS system and meteorological sensors, which were operated in parallel. The urban aerosol showed distinct bimodality with respect to both hygroscopic and volatile properties, which indicated that the urban aerosol contained an external mixture of particles with a diverse chemical composition. Vehicular road traffic had significant influence on both the hygroscopic and volatile properties, and contributed substantially to the particles in the NH and LV modes. These two modes were associated with each other, and both followed the typical diurnal pattern of road traffic and its workday/weekend variation. The other hygroscopic mode, i.e. the LH mode was composed of moderately transformed aged combustion particles consisting of partly oxygenated organics, inorganic salts and soot, and typically exhibited a volatility GF of approximately 0.6. Both the hygroscopic GFs and volatility GFs showed modest size dependent behaviour, while the fraction of particles in the modes exhibited much stronger size dependency. Smaller particle diameters were associated with a larger number fraction of non-volatile and hydrophobic particles than the larger diameters. This can be explained by assuming that the larger particles grew by condensation of organic vapours, and it is also supported by the small size dependency in the κ values with respect to the dry particle size. The 50-nm particles, however, had a considerably lower κ value and showed larger volatility during daytime in the LH mode with respect to the larger diameters. This suggests that these particles have a different chemical composition than the larger particles.

The transformation process of soot particles from hydrophobic to hydrophilic in the real atmosphere is still not sufficiently understood and constrained. The present study emphasizes the importance of the mixing state of particles on influencing their hygroscopic properties. The ambient conditions during the campaign were typical for wintertime Budapest. Since there are strong seasonal variations in both the anthropogenic and natural components, the hygroscopic and volatile properties are also expected to change. Therefore, further similar in situ measurements should be carried out in different seasons in the future together with on-line chemical characterisation of particles to better quantify and understand the properties, relevance and role of urban aerosol.

Atmospheric
Chemistry
and Physics
Discussions

Open Access

6 Data availability

The observational data used in this paper are available on request from J. E.

References

Baltensperger, U., Streit, N., Weingartner, E., Nyeki, S., Prévôt, A. S. H., Van Dingenen, R., Virkkula, A., Putaud, J.-P.,
Even, A., ten Brink, H., Blatter, A., Neftel, A., and Gäggeler, H. W.: Urban and rural aerosol characterization of summer
smog events during the PIPAPO field campaign in Milan, Italy, J. Geophys. Res., 107, 8193,
doi:10.1029/2001JD001292, 2002.

Bialek, J., Dall Osto, M., Vaattovaara, P., Decesari, S., Ovadnevaite, J., Laaksonen, A., and O'Dowd, C.: Hygroscopic and
chemical characterisation of Po Valley aerosol, Atmos. Chem. Phys., 14, 1557–1570, 2014.

Boucher, O., Randall, D., Artaxo, P., Bretherton, C., Feingold, G., Forster, P., Kerminen, V.-M., Kondo, Y., Liao, H.,
Lohmann, U., Rasch, P., Satheesh, S. K., Sherwood, S., Stevens, B., and Zhang, X. Y.: Clouds and Aerosols, in: Climate
Change 2013: The Physical Science Basis. Contribution of Working Group I to the Fifth Assessment Report of the
Intergovernmental Panel on Climate Change, edited by: Stocker, T. F., Qin, D., Plattner, G.-K., Tignor, M., Allen, S. K.,
Boschung, J., Nauels, A., Xia, Y., Bex, V., and Midgley, P. M., Cambridge University Press, Cambridge, UK, 571–658,
2013.

Brimblecombe, P.: Urban Pollution and Changes to Materials and Building Surfaces, Imperial College Press, London, 2016.

Chan, M. N. and Chan, C. K.: Mass transfer effects in hygroscopic measurements of aerosol particles, Atmos. Chem. Phys.,
2005.

Charron, A. and Harrison, R. M.: Primary particle formation from vehicle emissions during exhaust dilution in the roadside
atmosphere, Atmos. Environ., 37, 4109–4119, 2003.

Cocker, D., Whitlock, N., Flagan, R., and Seinfeld, J. H.: Hygroscopic properties of Pasadena, California aerosol, Aerosol
Sci. Technol., 35, 637–647, 2001.

Davidson, C. I., Phalen, R. F., and Solomon, P. A.: Airborne Particulate Matter and Human Health: A Review, Aerosol Sci.
Technol., 39, 737–749, 2005.

Duplissy, J., DeCarlo, P. F., Dommen, J., Alfarra, M. R., Metzger, A., Barmpadimos, I., Prévôt, A. S. H., Weingartner, E.,
Tritscher, T., Gysel, M., Aiken, A. C., Jimenez, J. L., Canagaratna, M. R., Worsnop, D. R., Collins, D. R., Tomlinson, J.,
and Baltensperger, U.: Relating hygroscopicity and composition of organic aerosol particulate matter, Atmos. Chem.
Phys., 11, 1155–1165, 2011.

Ehn, M., Petäjä, T., Aufmhoff, H., Aalto, P., Hämeri, K., Arnold, F., Laaksonen, A., and Kulmala, M.: Hygroscopic
properties of ultrafine aerosol particles in the boreal forest: diurnal variation, solubility and the influence of sulfuric acid,
Atmos. Chem. Phys., 7, 211–222, 2007.

Facchini, M. C., Mircea, M., Fuzzi, S., and Charlson, R. J.: Cloud albedo enhancement by surface-active organic solutes in
growing droplets, Nature, 401, 257–259, 1999.

Ferron, G. A., Karg, E., Busch, B., and Heyder, J.: Ambient particles at an urban, semi-urban and rural site in Central
Europe: Hygroscopic properties, Atmos. Environ., 39, 343–352, 2005.

Gysel, M., McFiggans, G. B., and Coe, H.: Inversion of tandem differential mobility analyser (TDMA) measurements, J.
Aerosol Sci., 40, 134–151, 2009.

Hakala, J., Mikkilä, J., Hong, J., Ehn, M., and Petäjä, T.: VH-TDMA: A description and verification of an instrument to measure aerosol particle hygroscopicity and volatility, Aerosol Sci. Technol., 51, 97–107, 2017.

Häkkinen, S. A. K., Äijälä, M., Lehtipalo, K., Junninen, H., Backman, J., Virkkula, A., Nieminen, T., Vestenius, M., Hakola, H., Ehn, M., Worsnop, D. R., Kulmala, M., Petäjä, T., and Riipinen, I.: Long-term volatility measurements of submicron
5   atmospheric aerosol in Hyytiälä, Finland, Atmos. Chem. Phys., 12, 10771–10786, 2012.

Henning, S., Ziese, M., Kiselev, A., Saathoff, H., Möhler, O., Mentel, T. F., Buchholz, A., Spindler, C., Michaud, V., Monier, M., Sellegri, K., and Stratmann, F.: Hygroscopic growth and droplet activation of soot particles: uncoated, succinic or sulfuric acid coated, Atmos. Chem. Phys., 12, 4525–4537, 2012.

Hong, J., Häkkinen, S. A. K., Paramonov, M., Äijälä, M., Hakala, J., Nieminen, T., Mikkilä, J., Prisle, N. L., Kulmala, M.,
10   Riipinen, I., Bilde, M., Kerminen, V. M., and Petäjä, T.: Hygroscopicity, CCN and volatility properties of submicron atmospheric aerosol in a boreal forest environment during the summer of 2010, Atmos. Chem. Phys., 14, 4733–4748, 2014.

Jurányi, Z., Tritscher, T., Gysel, M., Laborde, M., Gomes, L., Roberts, G., Baltensperger, U., and Weingartner, E.: Hygroscopic mixing state of urban aerosol derived from size-resolved cloud condensation nuclei measurements during
15   the MEGAPOLI campaign in Paris, Atmos. Chem. Phys., 13, 6431–6446, 2013.

Kamilli, K. A., Poulain, L., Held, A., Nowak, A., Birmili, W., and Wiedensohler, A.: Hygroscopic properties of the Paris urban aerosol in relation to its chemical composition, Atmos. Chem. Phys., 14, 737–749, 2014.

Kerminen, V.-M. and Wexler, A. S.: Growth laws of atmospheric aerosol particles: an examination of the bimodality of the accumulation mode, Atmos. Environ., 22, 3263–3275, 1995.

20   Kerminen, V.-M., Paramonov, M., Anttila, T., Riipinen, I., Fountoukis, C., Korhonen, H., Asmi, E., Laakso, L., Lihavainen, H., Swietlicki, E., Svenningsson, B., Asmi, A., Pandis, S. N., Kulmala, M., and Petäjä, T.: Cloud condensation nuclei production associated with atmospheric nucleation: a synthesis based on existing literature and new results. Atmos. Chem. Phys., 12, 12037–12059, 2012.

Kitamori, Y., Mochida, M., and Kawamura, K.: Assessment of the aerosol water content in urban atmospheric particles by
25   the hygroscopic growth measurements in Sapporo, Japan, Atmos. Environ., 43, 3416–3423, 2009.

Kulmala, M., Petäjä, T., Nieminen, T., Sipilä, M., Manninen, H. E., Lehtipalo, K., Dal Maso, M., Aalto, P. P., Junninen, H., Paasonen, P., Riipinen, I., Lehtinen, K. E. J., Laaksonen, A., and Kerminen, V.-M.: Measurement of the nucleation of atmospheric aerosol particles, Nat. Protocols, 7, 1651–1667, 2012.

Laborde, M., Crippa, M., Tritscher, T., Jurányi, Z., Decarlo, P. F., Temime-Roussel, B., Marchand, N., Eckhardt, S., Stohl,
30   A., Baltensperger, U., Prévôt, A. S. H., Weingartner, E., and Gysel, M.: Black carbon physical properties and mixing state in the European megacity Paris, Atmos. Chem. Phys., 13, 5831–5856, 2013.

Lance, S., Raatikainen, T., Onasch, T. B., Worsnop, D. R., Yu, X. Y., Alexander, M. L., Stolzenburg, M. R., McMurry, P. H., Smith, J. N., and Nenes, A.: Aerosol mixing state, hygroscopic growth and cloud activation efficiency during MIRAGE 2006, Atmos. Chem. Phys., 13, 5049–5062, 2013.

35   Lelieveld, J., Evans, J. S., Fnais, M., Giannadaki, D., and Pozzer, A.: The contribution of outdoor air pollution sources to premature mortality on a global scale, Nature, 525, 367–71, 2015.

Liu, P. F., Zhao, C. S., Göbel, T., Hallbauer, E., Nowak, A., Ran, L., Xu, W. Y., Deng, Z. Z., Ma, N., Mildenberger, K., Henning, S., Stratmann, F., and Wiedensohler, A.: Hygroscopic properties of aerosol particles at high relative humidity and their diurnal variations in the North China Plain, Atmos. Chem. Phys., 11, 3479–3494, 2011.

40   Liu, D., Allan, J., Whitehead, J., Young, D., Flynn, M., Coe, H., McFiggans, G., Fleming, Z. L., and Bandy, B.: Ambient black carbon particle hygroscopic properties controlled by mixing state and composition, Atmos. Chem. Phys., 13, 2015–2029, 2013.

Martin, M., Tritscher, T., Jurányi, Z., Heringa, M. F., Sierau, B., Weingartner, E., Chirico, R., Gysel, M., Prévôt, A. S. H., Baltensperger, U., and Lohmann, U.: Hygroscopic properties of fresh and aged wood burning particles, J. Aerosol Sci., 56, 15–29, 2012.

Massoli, P., Lambe, A. T., Ahern, A. T., Williams, L. R., Ehn, M., Mikkilä, J., Canagaratna, M. R., Brune, W. H., Onasch, T. B., Jayne, J. T., Petäjä, T., Kulmala, M., Laaksonen, A., Kolb, C. E., Davidovits, P., and Worsnop, D. R.: Relationship between aerosol oxidation level and hygroscopic properties of laboratory generated secondary organic aerosol (SOA) particles, Geophys. Res. Lett., 37, L24801, doi:10.1029/2010GL045258, 2010.

Massling, A., Stock, M., and Wiedensohler, A.: Diurnal, weekly, and seasonal variation of hygroscopic properties of submicrometer urban aerosol particles, Atmos. Environ., 39, 3911–3922, 2005.

Massling, A., Niedermeier, N., Hennig, T., Fors, E. O., Swietlicki, E., Ehn, M., Hämeri, K., Villani, P., Laj, P., Good, N., McFiggans, G., and Wiedensohler, A.: Results and recommendations from an intercomparison of six Hygroscopicity-TDMA systems, Atmos. Meas. Tech., 4, 485–497, 2011.

McFiggans, G., Artaxo, P., Baltensperger, U., Coe, H., Facchini, M. C., Feingold, G., Fuzzi, S., Gysel, M., Laaksonen, A., Lohmann, U., Mentel, T. F., Murphy, D. M., O'Dowd, C. D., Snider, J. R., and Weingartner, E.: The effect of physical and chemical aerosol properties on warm cloud droplet activation, Atmos. Chem. Phys., 6, 2593–2649, 2006.

McMurry, P. and Stolzenburg, M.: On the sensitivity of particle size to relative humidity for Los Angeles aerosols, Atmos. Environ., 23, 497–507, 1989.

Meng, Z. and Seinfeld, J. H.: On the source of the submicrometer droplet mode of urban and regional aerosols, Aerosol Sci. Technol., 20, 253–265, 1994.

Mercado, L., Bellouin, N., Sitch, S., Boucher, O., Huntingford, C., Wild, M., and Cox, P. M.: Impact of changes in diffuse radiation on the global land carbon sink, Nature, 458, 1014–1017, 2009.

Mircea, M., Facchini, M. C., Decesari, S., Cavalli, F., Emblico, L., Fuzzi, S., Vestin, A., Rissler, J., Swietlicki, E., Frank, G., Andreae, M. O., Maenhaut, W., Rudich, Y., and Artaxo, P.: Importance of the organic aerosol fraction for modeling aerosol hygroscopic growth and activation: a case study in the Amazon Basin, Atmos. Chem. Phys., 5, 3111-3126, 2005.

Németh, Z., Pósfai, M., Nyirő-Kósa, I., Aalto, P., Kulmala, M., and Salma, I.: Images and properties of individual nucleated particles, Atmos. Environ., 123, 166–170, 2015.

Park, K., Kim, J–S., and Park, S. H.: Measurements of hygroscopicity and volatility of atmospheric ultrafine particles during ultrafine particle formation events at urban, industrial, and coastal sites, Environ. Sci. Technol., 43, 6710–6716, 2009.

Petters, M. D. and Kreidenweis, S. M.: A single parameter representation of hygroscopic growth and cloud condensation nucleus activity, Atmos. Chem. Phys., 7, 1961–1971, 2007.

Pringle, K. J., Tost, H., Pozzer, A., Pöschl, U., and Lelieveld, J.: Global distribution of the effective aerosol hygroscopicity parameter for CCN activation, Atmos. Chem. Phys., 10, 5241-5255, 2010.

Raes, F., Van Dingenen, R., Vignati, E., Wilson, J., Putaud, J. P., Seinfeld, J. H., and Adams, P.: Formation and cycling of aerosol in the global troposphere. Atmos. Environ., 34, 4215–4240, 2000.

Rissler, J., Pagels, J., Swietlicki, E., Wierzbicka, W., Strand, M., Lillieblad, L., Sanati, M., and Bohgard, M.: Hygroscopic behavior of aerosol particles emitted from biomass fired grate boilers, Aerosol Sci. Technol., 39, 919–930, 2005.

Rissler, J., Svenningsson, B., Fors, E. O., Bilde, M., and Swietlicki, E.: An evaluation and comparison of cloud condensation nucleus activity models: Predicting particle critical saturation from growth at subsaturation, J. Geophys. Res., 115, D22208, doi:10.1029/2010jd014391, 2010.

Salma, I., Ocskay, R., Varga, I., and Maenhaut, W.: Surface tension of atmospheric humic-like substances in connection with relaxation, dilution, and solution pH, J. Geophys. Res., 111, D23205, doi:10.1029/2005JD007015, 2006.

Salma, I., Borsós, T., Aalto, P., and Kulmala, M.: Time-resolved number concentrations and size distribution of aerosol particles in an urban road tunnel, Boreal Environment Research, 16, 262–272, 2011a.

Atmospheric
Chemistry
and Physics
Discussions

Salma, I., Borsós, T., Weidinger, T., Aalto, P., Hussein, T., Dal Maso, M., and Kulmala, M.: Production, growth and properties of ultrafine atmospheric aerosol particles in an urban environment, Atmos. Chem. Phys., 11, 1339–1353, 2011b.

Salma, I., Borsós, T., Németh, Z., Weidinger, T., Aalto, T., and Kulmala, M.: Comparative study of ultrafine atmospheric
5   aerosol within a city, Atmos. Environ., 92, 154–161, 2014.

Salma, I., Németh, Z., Weidinger, T., Kovács, B., and Kristóf, G.: Measurement, growth types and shrinkage of newly formed aerosol particles at an urban research platform, Atmos. Chem. Phys., 16, 7837–7851, 2016a.

Salma, I., Németh, Z., Kerminen, V. M., Aalto, P., Nieminen, T., Weidinger, T., Molnár, Á., Imre, K., and Kulmala, M.: Regional effect on urban atmospheric nucleation, Atmos. Chem. Phys., 16, 8715–8728, 2016b.

10   Salma, I., Németh, Z., Weidinger, T., Maenhaut, W., Claeys, M., Molnár, M., Major, I., Ajtai, T., Utry, N., and Bozóki, Z.: Source apportionment of carbonaceous chemical species to fossil fuel combustion, biomass burning and biogenic emissions by a coupled radiocarbon-levoglucosan marker method, Atmos. Chem. Phys. Discuss., doi:10.5194/acp-2017-406, in review, 2017.

Swietlicki, E., Hansson, H. C., Hämeri, K., Svenningsson, B., Massling, A., McFiggans, G., McMurry, P. H., Petäjä, T.,
15   Tunved, P., Gysel, M., Topping, D., Weingartner, E., Baltensperger, U., Rissler, J., Wiedensohler, A., and Kulmala, M.: Hygroscopic properties of submicrometer atmospheric aerosol particles measured with H-TDMA instruments in various environments – a review, Tellus B, 60, 432–469, 2008.

Tiitta, P., Miettinen, P., Vaattovaara, P., Joutsensaari, J., Petäjä, T., Virtanen, A., Raatikainen, T., Aalto, P., Portin, H., Romakkaniemi, S., Kokkola, H., Lehtinen, K. E. J., Kulmala, M., and Laaksonen, A.: Roadside aerosol study using
20   hygroscopic, organic and volatility TDMAs: Characterization and mixing state, Atmos. Environ., 44, 976–986, 2010.

Tritscher, T., Jurányi, Z., Martin, M., Chirico, R., Gysel, M., Heringa, M. F., DeCarlo, P. F., Sierau, B., Prévôt, A. S. H., Weingartner, E., and Baltensperger, U.: Changes of hygroscopicity and morphology during ageing of diesel soot, Environ. Res. Let., 6, 10.1088/1748-9326/6/3/034026, 2011.

Ye, X., Tang, C., Yin, Z., Chen, J., Ma, Z., Kong, L., Yang, X., Gao, W., and Geng, F.: Hygroscopic growth of urban aerosol
25   particles during the 2009 Mirage-Shanghai Campaign, Atmos. Environ., 64, 263–269, 2013.

Weingartner, E., Baltensperger, U., and Burtscher, H.: Growth and structural change of combustion aerosols at high relative humidity. Environ, Sci. Technol., 29, 2982–2986, 1995.

Weingartner, E., Burtscher, H., and Baltensperger, U.: Hygroscopic properties of carbon and diesel soot particles, Atmos. Environ., 31, 2311–2327, 1997.

30   Wiedensohler, A., Cheng, Y. F., Nowak, A., Wehner, B., Achtert, P., Berghof, M., Birmili, W., Wu, Z. J., Hu, M., Zhu, T., Takegawa, N., Kita, K., Kondo, Y., Lou, S. R., Hofzumahaus, A., Holland, F., Wahner, A., Gunthe, S. S., Rose, D., Su, H., and Pöschl, U.: Mobility particle size spectrometers: harmonization of technical standards and data structure to facilitate high quality long-term observations of atmospheric particle number size distributions. Atmos. Meas. Tech., 5, 657–685, 2012.

35   Wu, Z. J., Zheng, J., Shang, D. J., Du, Z. F., Wu, Y. S., Zeng, L. M., Wiedensohler, A., and Hu, M.: Particle hygroscopicity and its link to chemical composition in the urban atmosphere of Beijing, China, during summertime, Atmos. Chem. Phys., 16, 1123–1138, 2016.